NICOLAUS COPERNICUS UNIVERSITY IN TORUŃ

Bulletin of Geography. Physical Geography Series, No. 29 (2025): 23–41
http://doi.org/10.12775/bgeo-2025-0008

Assessing Land Use and Land Cover changes in Al Hoceima province, Morocco (2014–2024): a comparative analysis using machine learning algorithms

Morad Taher[1*] [a], Mariem Ben-Said[2] [b], Abdelhak Bourjila[3] [c], Ali Errahmouni[4] [d], Alae Mouddou[1] [e], Issam Etebaai[1]

[1]Abdelmalek Essaâdi University, Research and Development in Applied Geosciences Laboratory, FSTT, Tetouan, Morocco
[2]Abdelmalek Essaâdi University, Laboratory of Biology, Ecology and Health, Department of Biology, FS of Tetouan, Tetouan, Morocco
[3]Abdelmalek Essaâdi University, Laboratory of Engineering Sciences and Applications (LSIA)- Research team: Materials Science, Energy and Environment (SM2E), ENSAH, Tetouan, Morocco
[4]Abdelmalek Essaâdi University, Department of Geology, FS of Tetouan, Tetouan, Morocco

*Correspondence e-mail: m.taher@uae.ac.ma

[a]https://orcid.org/0000-0002-9273-2764, [b]https://orcid.org/0000-0002-5171-0542, [c]https://orcid.org/0000-0003-2592-6179, [d]https://orcid.org/0000-0003-0303-8971, [e]https://orcid.org/0009-0004-9444-6659

Abstract. The present work employed remote sensing data (Landsat 8 OLI images), two machine learning algorithms (Random Forest (RF) and Support Vector Machine (SVM)) and a parametric algorithm (Maximum Likelihood – MLH) within the ArcGIS environment to assess the spatiotemporal Land Use and Land Cover changes in Al Hoceima province (north-eastern Morocco) from 2014 to 2024. Based on the classification generated by the MLH algorithm, there were increases in the forest, urban area and water/river classes of 8.2%, 1.2% and 0.2%, respectively. Conversely, the vegetation and bare land classes decreased by 1% and 8%, respectively. The RF indicated that the forest and water/river classes remained stable from 2014 to 2024, vegetation decreased by 2.3%, while urban area and bare land increased by 0.6% and 1% respectively. The SVM classification revealed an increase of 1% and 0.8% in the forest and urban area, respectively. However, water/river, vegetation and bare land decreased by 0.2%, 1% and 0.2%, respectively. Overall, there were two common trends for the three classifiers: an increase in urban area (of between 0.6% and 1.2 %) and a decrease in vegetation (of between –1% for both MLH and SVM and –2.3% for RF). In terms of accuracy evaluation, the MLH exhibits remarkable overall accuracy of 91% and Kappa coefficient (K = 0.89) followed by the SVM with 88% (K = 0.84). To validate the outcomes of the three algorithms classifier, an estimation of the Normalized Difference Vegetation Index (NDVI) changes was conducted. The results of NDVI changes support the outcomes of the RF classifier, although it gave the lowest accuracy, with 81% (K = 0.77).

Key words:
GIS,
Landsat,
Maximum Likelihood,
NDVI,
Rif,
Remote Sensing,
Random Forest
Support Vector Machine

Introduction

Analyzing the Globe's surface alterations is a key step to understanding socio-ecological shifts (Atef et al. 2023). Globally, Land Use and Land Cover (LULC) is highly dynamic due to human activities and extensive land development, such as urbanization, artisanal mining and expansion of vegetation (Gxokwe et al. 2023; Kruasilp et al. 2023). According to Shetty et al. (2021) and Chaves

et al. (2020), "land cover" pertains to the physical elements covering the Earth's surface, whereas "land use" denotes the purpose for which the land is employed. Nowadays, the systematic review highlights the growing potential of using Landsat 8 and Sentinel-2 data for accurate LULC mapping and change detection, particularly in agriculture and natural vegetation (Chaves et al. 2020).

The effectiveness of LULC examination has been enhanced through the integration of various image classification methods. These include the maximum likelihood (Mirmazloumi et al. 2022; Ait El Haj et al. 2023), parallelepiped (Alshari and Gawali 2021), minimum distance (Dibs et al. 2020), linear discriminant (Wulder et al. 2018b) and Bayesian (Hasan et al. 2023) for parametric classifiers. Machine learning classifiers, such as Support Vector Machines (Adam et al. 2014), random forest (Phan et al. 2020), and k-nearest neighbor (Chirici et al. 2016) have also been employed, in addition to deep learning classifiers such as artificial neural networks (Sisay et al. 2023) and convolutional neural networks (Kumar and Kumar Gorai 2023). Numerous studies have focused on comparing the accuracy of these methods, as well as RS products, such as those conducted by Chowdhury (2024a) and Wang et al. (2023). The most popular and widely employed in the field of LULC mapping are: among the parametric classifiers, Maximum Likelihood (MLH); and among machine learning classifiers, Random Forest (RF) and Support Vector Machines (SVM) (Wang et al. 2023).

Several studies in Morocco have employed diverse RS data and classification techniques for LULC analysis (Ben-Said et al. 2025). For example, Mohajane et al. (2018) employed the RF classification using a multispectral Scanner (MSS), Thematic Mapper (TM), Enhanced Thematic Mapper Plus (ETM+) and Operational Land Imager OLI images to describe the vegetation change of Azrou Forest in the central middle Atlas between 1987 and 2017. The authors indicated that the overall forest cover remained constant. Nguyen et al. (2023) utilized the SVM classification of LULC using Landsat data spanning from the 1990s to the 2020s to differentiate between open-canopy vegetation, bare land, forest and water in the High Atlas Mountains. In the Lakhdar sub-basin, province of Beni-Mellal, Ait El Haj et al. (2023) employed the MLH classification using multi-temporal RS data, encompassing Landsat images such as Landsat 7 (ETM+), Landsat 5 (TM), and Landsat 8 (OLI) captured between 2000 and 2020 to observe land cover changes in the sub-basin.

LULC maps provide valuable insights into the relationship between human activities and the natural environment, helping to understand the evolving landscape (Mirmazloumi et al. 2022). Assessing LULC changes is essential for addressing population growth, industrial development, and their environmental impacts, especially in emerging countries (Ienco et al. 2019). These maps are crucial for mitigating global warming and for land use planning (Lavanya et al. 2023), with various models available to simulate LULC patterns and the influence of human activities (Mansour et al. 2023).

Early LULC mapping relied on field surveys and manual visual interpretation, which were costly and ineffective for regular monitoring (Wulder et al. 2018a; Dibs et al. 2020). The rise of global urbanization and its impacts have highlighted the importance of geospatial methods for tracking and predicting spatio-temporal LULC changes, enhancing understanding of land alterations and their spatial implications (Adam et al. 2014; Hasan et al. 2023). In the modern era, remote sensing (RS) technology has advanced significantly, leveraging big data to collect invaluable datasets for various applications. These include monitoring hazards and natural disasters (Taher et al. 2022), prediction of salinity (Bourjila et al. 2023), groundwater mapping (Bourjila et al. 2021; Errahmouni et al. 2022; Taher et al. 2023), LULC mapping (Lekka et al. 2024) and soil erosion assessment (Taher et al. 2022), contributing significantly to nature conservation (Daunt et al. 2021) and monitoring of natural resources (Verde et al. 2020).

The classification of RS images from spaceborne or aerial platforms remains the primary method for discerning LULC types (Shetty et al. 2021). The accessibility of medium spatial resolution satellite imagery, such as Landsat 8, enables the development of detailed and cost-effective land cover datasets at national and supra-national scales (Verde et al. 2020). While RS offers significant advantages, the inclusion of in-situ data is crucial for achieving high accuracy in supervised classification methods (Chaves et al. 2020). Recent RS research integrates artificial intelligence techniques, including machine learning and deep learning, to extract more discriminative features, enhance satellite image

classification and extract valuable information (Pandey et al. 2023).

The province of Al Hoceima is undergoing significant environmental and socio-economic changes, influenced by factors such as climate change, recurring droughts and rapid population growth (Bourjila et al. 2020). It is expected that ongoing and future studies will confirm that substantial transformations in LULC have occurred over the past decade. However, the evidence for these changes remains sparse, particularly regarding the expansion of urban and barren areas at the expense of green spaces like forests and vegetation (Chu 2022). The lack of comprehensive studies in this region creates a substantial research gap, as the impacts of these dynamic processes on LULC have not been systematically analyzed.

This study specifically aims to fill this gap by investigating the LULC changes in Al Hoceima over a ten-year period (2014–2024), focusing on two key objectives: 1) to assess the extent and nature of these changes, and 2) to evaluate the effectiveness of three widely used classification methods – namely, Random Forest (RF), Support Vector Machine (SVM), and Maximum Likelihood (MLH) – for accurately mapping LULC. By applying Landsat 8 satellite imagery, this study not only provides an empirical assessment of LULC changes in the region but also presents a comparative analysis of the classification techniques commonly employed in remote sensing studies.

Addressing the identified gap in LULC knowledge, this study contributes by providing evidence of how LULC has evolved in the context of climate change and population growth, which are major drivers of land use transformations. The comparative analysis of the three classifiers offers a critical insight into the most effective methods for mapping LULC in this region, taking into account the unique challenges posed by Al Hoceima's diverse and complex landscape.

In order to ensure the robustness of the results, the study employs multiple accuracy assessment metrics, including the kappa coefficient (K), overall accuracy (OA), user's accuracy (UA) and producer's accuracy (PA). These metrics provide a reliable evaluation of the classification methods, ensuring the reliability of the study's findings. Furthermore, the most accurate method identified in the initial evaluation was subjected to additional validation using the Normalized Difference Vegetation Index (NDVI), a tool that provides further verification of the classification's effectiveness, particularly in distinguishing vegetation and land cover types.

In sum, this study makes significant contributions to the understanding of LULC changes in Al Hoceima by addressing the existing research gap, presenting a comparative analysis of classification methods, and validating the findings through a comprehensive set of accuracy assessments. These efforts provide valuable insights for future studies on land use planning, environmental conservation and policy formulation in regions facing similar environmental and socio-economic challenges.

Materials and methods

Study area

Al Hoceima province (Fig. 1), located along the Mediterranean coast of north-eastern Morocco, lies within the Rif Mountain range between latitudes 35°25'–34°66'N and longitudes 3°80'–4°81'W. Spanning 3,550 km², it is part of the Tanger-Tetouan-Al Hoceima region and bordered by the Mediterranean Basin to the north, Taza and Taounate provinces to the south, Driouch province to the east, and Chefchaouen province to the west. The province encompasses 36 communes, including the urban centers of Al Hoceima, Imzouren, Bni Bouayach, Ajdir and Targuist. Known for its diverse landscapes, it features mountains, beaches, forests (such as Boujibar, Swani-Sfiha, Chakran and Sanhaja) and Jbel Tidghine, the highest summit in the Rif range at 2,452 m a.s.l. The province experiences a semiarid Mediterranean climate with cold winters (average 10 °C) and hot summers (average 28.5°C). Annual rainfall ranges from 250 mm to 500 mm, averaging 300 mm, but can reach up to 1,000 mm at higher altitudes (HCP 2017).

According to the last Moroccan General Census of Population and Housing carried out in 2024, the total population of the province is 371.527, with 62.6% in rural areas. In the study area, the main human activities are agriculture (cereal crops with almond trees), grazing, fishing, and crafts (including women's pottery, basketry and traditional weaving), as well tourism (HCP 2017).

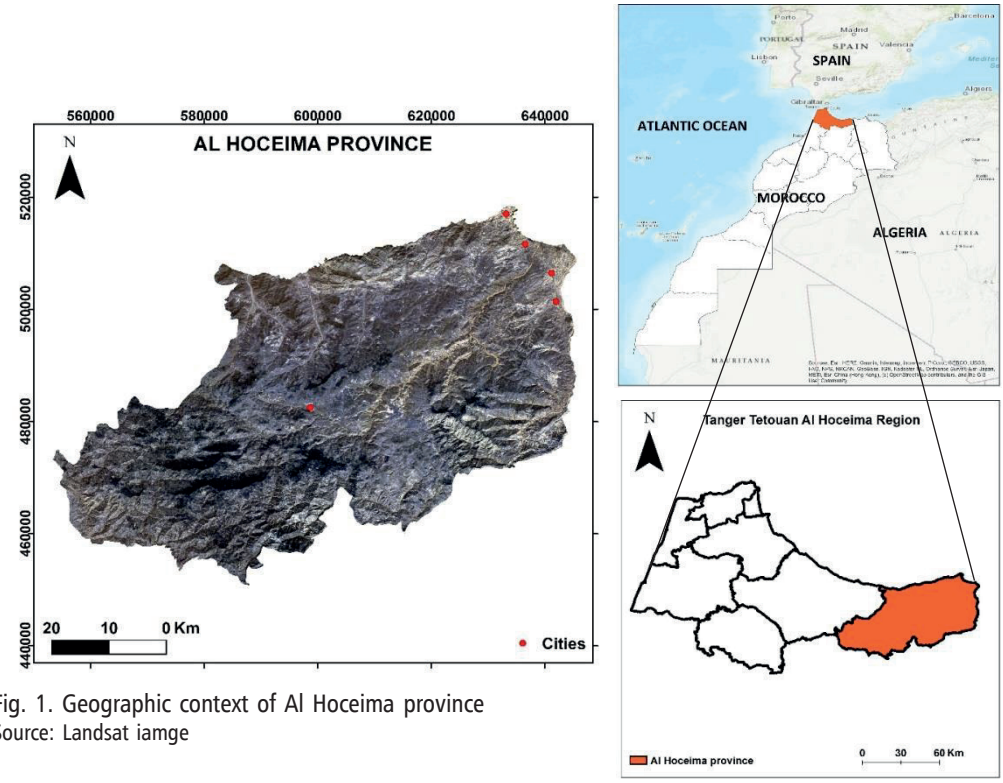

Fig. 1. Geographic context of Al Hoceima province
Source: Landsat iamge

In Al Hoceima province, surface water resources are scarce; the rivers, which drain relatively small catchments, are mostly seasonal and thus, mainly during the summer, are dry. These rivers are: Oued Feddal, O. Beni Boufrah, O. Badès (Al-Aansar), O. Boussekour and O. Snada (HCP 2017). Geologically, Al Hoceima province is located on the border between the African and Eurasian plates (Taher et al. 2023). Consequently, it is characterized by tectonic and seismic activities such as the Mw 6.0 earthquake of May 26, 1994, the Mw 6.4 earthquake of February 24, 2004 and the Mw 6.4 earthquake of January 25, 2016 (Gislason et al. 2006; Tassi et al. 2021). The soils are dominated by impermeable or poorly permeable substrate (shales and marls), which generally explains the scarcity of underground water resources (HCP 2017). With 70% of the soil affected by erosion, the Rif region is considered one of the most eroded in the world. Tectonic activity and soil erosion significantly impact LULC changes by altering topography, soil stability and ecological systems (Gong 2022). Tectonic processes such as uplift and earthquakes reshape terrains, disrupt infrastructure and modify water drainage, influencing land suitability for agriculture, urban development and conservation. Soil erosion depletes fertile land, causes sedimentation in water bodies and leads to vegetation loss, further degrading ecosystems. These factors often result in shifts in agricultural practices, land abandonment or changes to less-intensive uses like forestry. Additionally, conservation efforts, such as reforestation and protected zones, are often implemented to counteract these effects, driving further changes in LULC patterns.

Al Hoceima holds significant importance in the Rif region, hosting one of the key Mediterranean ports and the only protected area on Morocco's Mediterranean coast: the Al Hoceima National Park, established in 2004. Spanning 48,460 ha (including 19,000 ha of marine zones), the park aims to preserve its marine biodiversity, fisheries, agro-sylvo-pastoral heritage and cultural landscapes. Its rich woody vegetation includes species such as Berber thuja, Aleppo pine, wild olive and holm oak, while its diverse fauna features emblematic species like the osprey and Audouin's gull, making the park a crucial habitat for bird migration, nesting and resting (UICN 2012; HCP 2017).

Citation: Bulletin of Geography. Physical Geography Series 2025, 29, http://doi.org/10.12775/bgeo-2025-0008

Table 1. The Landsat 8 data information used in the present study

Date Acquired	ID	Path	Row	Cloud cover	Band used
17/10/2014	LC08_L1TP_200036_20141017_20200910_02_T1	200	036	0.00 %	7
14/01/2024	LC08_L1TP_200036_20240114_20240114_02_RT_	200	036	16.72 %	7

Data and pre-processing

Landsat 8 images from two dates, 2014 and 2024, were utilized in the study (Table 1). The period from 2014 to 2024 was selected for several reasons. Firstly, it offers a recent and relevant timeframe for assessing changes in land use and land cover, reflecting contemporary environmental and socio-economic dynamics. Secondly, the availability of clear, cloud-free imagery for these years allowed us to maintain consistency and accuracy in our analysis. Lastly, this period captures a decade of significant environmental changes around the globe, including the impacts of climate change, urbanization and land management practices, making it a robust timeframe for our study. The Landsat 8 satellite, downloaded from the United States Geological Survey (USGS) website using cloud and date filtering, is equipped with two sensors: the Operational Land Imager (OLI) providing 30-m spatial resolution and nine bands, and the Thermal InfraRed Sensor (TIRS) offering 100-m spatial resolution and two bands (Mirmazloumi et al. 2022). These thermal bands are primarily used to detect and monitor temperature variations on Earth's surface, offering valuable insights for various applications, such as monitoring water bodies and vegetation. The decision to employ Landsat 8 data is tied to the potential for conducting a subsequent comprehensive analysis of long-term LULC changes using earlier Landsat data (Tassi et al. 2021). In mountainous areas, such as the study area, the surface reflectance is significantly impacted by the topography, particularly because of the steep slopes (Tassi et al. 2021). Therefore, radiometric correction is applied to Landsat images to reduce the topographic effect.

Training samples

Using natural-color Landsat images, 455 samples well distributed throughout the Al Hoceima province were selected manually as training samples for the year 2014, and 458 for the year 2024. Furthermore, utilizing ArcGIS software, for each land cover class, multiple samples were selected to ensure accurate and representative results. In each class, we systematically collected several samples to cover the spatial heterogeneity of the study area as comprehensively as possible. This approach was designed to account for variations within each class and enhance the robustness of the classification process. Google Earth Pro was employed as an auxiliary source to validate the accuracy of the selected training samples. This tool provided high-resolution imagery that allowed for better assessment and validation of the sample locations, ensuring that the samples were accurately aligned with ground realities. The distribution of training samples per class is detailed in Table 2.

Table 2. Training samples for each LULC

Years	2014	2024
Classes	Training samples	
Forest	87	85
Urban Area	40	42
Water/River	110	110
Vegetation	60	60
Bare Land	60	63

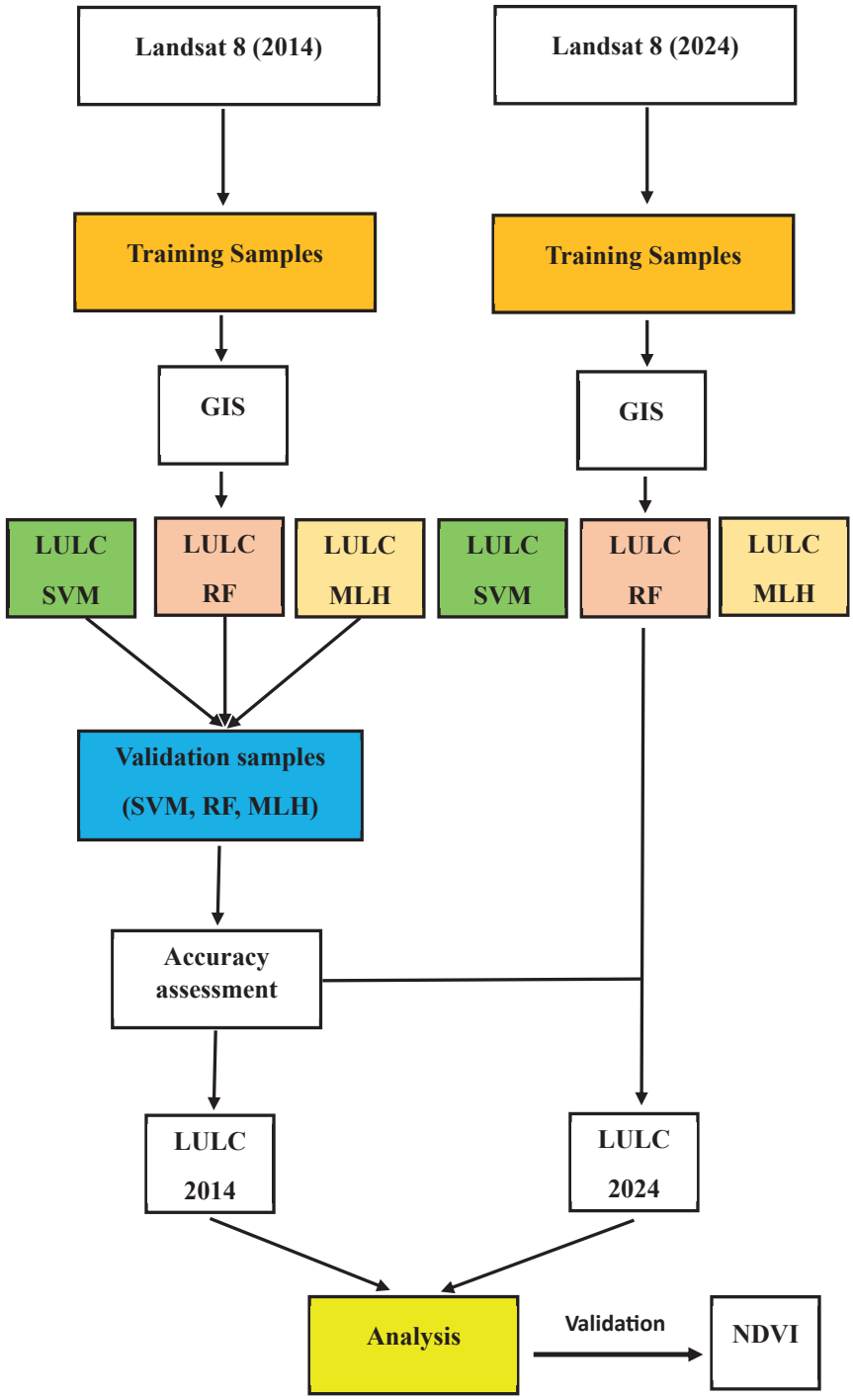

Fig. 2. Flowchart of methodology adopted for the current study

Classification algorithms (RF, MLH, SVM)

This study compared two machine learning algorithms, namely Random Forest (RF) and Support Vector Machine (SVM), alongside one parametric algorithm, the Maximum Likelihood Classifier (MLH). Figure 2 shows the flowchart of the methodology adopted for the current study.

Citation: Bulletin of Geography. Physical Geography Series 2025, 29, http://doi.org/10.12775/bgeo-2025-0008

- RF, a conventional machine learning algorithm, is one of the most robust and generally used techniques of supervised classification for LULC monitoring (Gislason et al. 2006). Furthermore, it is a powerful non-parametric statistical model used to handle non-linear relations (Kruasilp et al. 2023).
- SVM, a supervised learning technique, is employed to address various regression and classification-related challenges (Basheer et al. 2022). Furthermore, SVM stands as a prevalent machine learning algorithm extensively applied in RS image classification, yielding higher accuracy in multi-temporal satellite image classification (Chowdhury 2024b).
- MLH is a parametric classifier widely used in LULC classification (Chowdhury 2024b). It is a supervised classification method that describes every band by a normal distribution (Basheer et al. 2022). Many researchers select this classic algorithm to assess the accuracy of other algorithms (Chowdhury 2024b). The Maximum Likelihood Classifier (MLC) is included in this study as a baseline for comparison, given its historical significance and frequent use in earlier LULC studies. By evaluating its performance alongside advanced non-parametric algorithms, we aim to demonstrate the advantages of modern methods over traditional approaches. This comparison provides a comprehensive perspective on algorithmic advancements.

Accuracy Assessment

Accuracy assessment of LULC classification of Al Hoceima province was performed using the confusion matrix (Kruasilp et al. 2023), which served as the basis for calculating several performance metrics, including the kappa coefficient (K), overall accuracy (OA), user's accuracy (UA), and producer's accuracy (PA). We chose the OA and K as the primary accuracy indicators for evaluating the precision and efficiency of all classifiers, given their frequent preference in assessment (Junaid et al. 2023). OA represents the percentage of correctly classified validation data (Basheer et al. 2022). Furthermore, K was calculated to assess the accuracy of each classifier utilized for the year 2014. A greater K value (from 0.8 to 1.0) indicates the optimal arrangement of raster data, reflecting enhanced efficiency in LULC classification (McHugh 2012). Unlike overall accuracy, UA and PA provide specific insight into the accuracy of individual categories. UA reflects the accuracy of classified pixels from the user's viewpoint, representing the proportion of correctly classified pixels compared to the ground reality. On the other hand, PA measures accuracy from the producer's perspective, indicating the percentage of ground truth pixels correctly identified within the classification results (Atef et al. 2023). Hence, a high-resolution image from Google Earth was employed to validate the accuracy of each class's validation samples (Table 3) and the generated LULC maps (Fig. 3) resulting from the classification algorithms. Equations (1), (2), (3) and (4) illustrate the method for calculating OA, K, UA and PA, respectively (Basheer et al. 2022).

Table 3. Validation samples of each LULC class and each algorithm classification for the year 2014 using Google Earth

Year	2014		
Classes	Validation samples		
	MLH	RF	SVM
Forest	70	68	69
Urban Area	30	29	25
Water/River	62	64	67
Vegetation	39	44	37
Bare Land	66	60	67

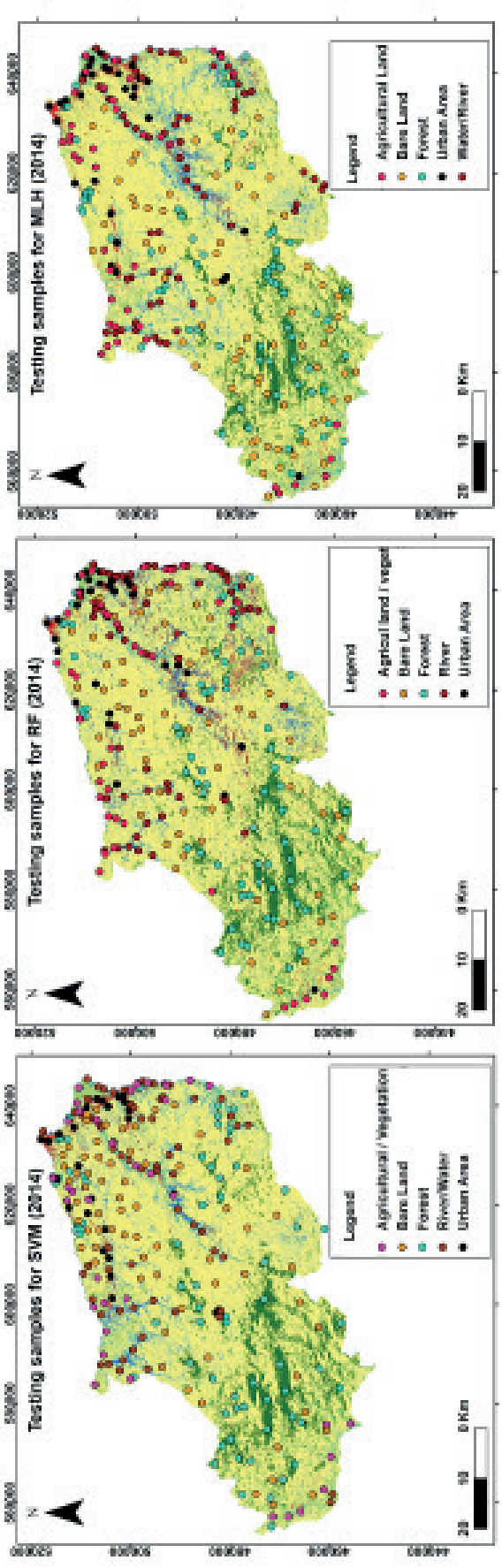

Fig. 3. The location of validation samples on LULC maps

$$OA = (Tcvs \div Tvs) \times 100$$

where OA is the overall accuracy, T_{cvs} is the total number of correctly validated samples and T_{vs} is the total number of validation samples.

$$KC = (OA - CA) \div (1 - CA)$$

where KC is kappa coefficient and CA is the chance agreement.

$$UA = (n_{ii} / n_{+i}) \times 100$$

$$PA = (n_{ii} / n_{+i}) \times 100$$

where n_{ii} and n_{+i} represent the marginal sum of rows and columns, respectively.

Normalized Difference Vegetation Index

The NDVI was mapped to quantify vegetation changes from 2014 to 2024 in the study area, utilizing the Landsat 8 images. This vegetation index is extensively employed and offers insights into the quantity and vitality of vegetation, taking into account the near-infrared reflectance (NIR) and the reflectance in the red band (RED) (Abdelkarim 2023; Frimpong et al. 2023; Hossain et al. 2023; Hu et al. 2023). The scale of NDVI spans from –1 to 1, where a negative value denotes areas devoid vegetation, whereas a positive value indicates the presence of vegetation (Junaid et al. 2023). In the current study, the NDVI is employed to evaluate the LULC outcomes of algorithmic classifiers, with a particular focus on the forest and bare land classes. The NDVI is calculated using the following equation:

Results

LULC analysis

The present study investigates the changes in LULC between 2014 and 2024 in Al Hoceima province. The LULC maps employed in this research were generated utilizing Landsat satellite data and

Citation: Bulletin of Geography. Physical Geography Series 2025, 29, http://doi.org/10.12775/bgeo-2025-0008

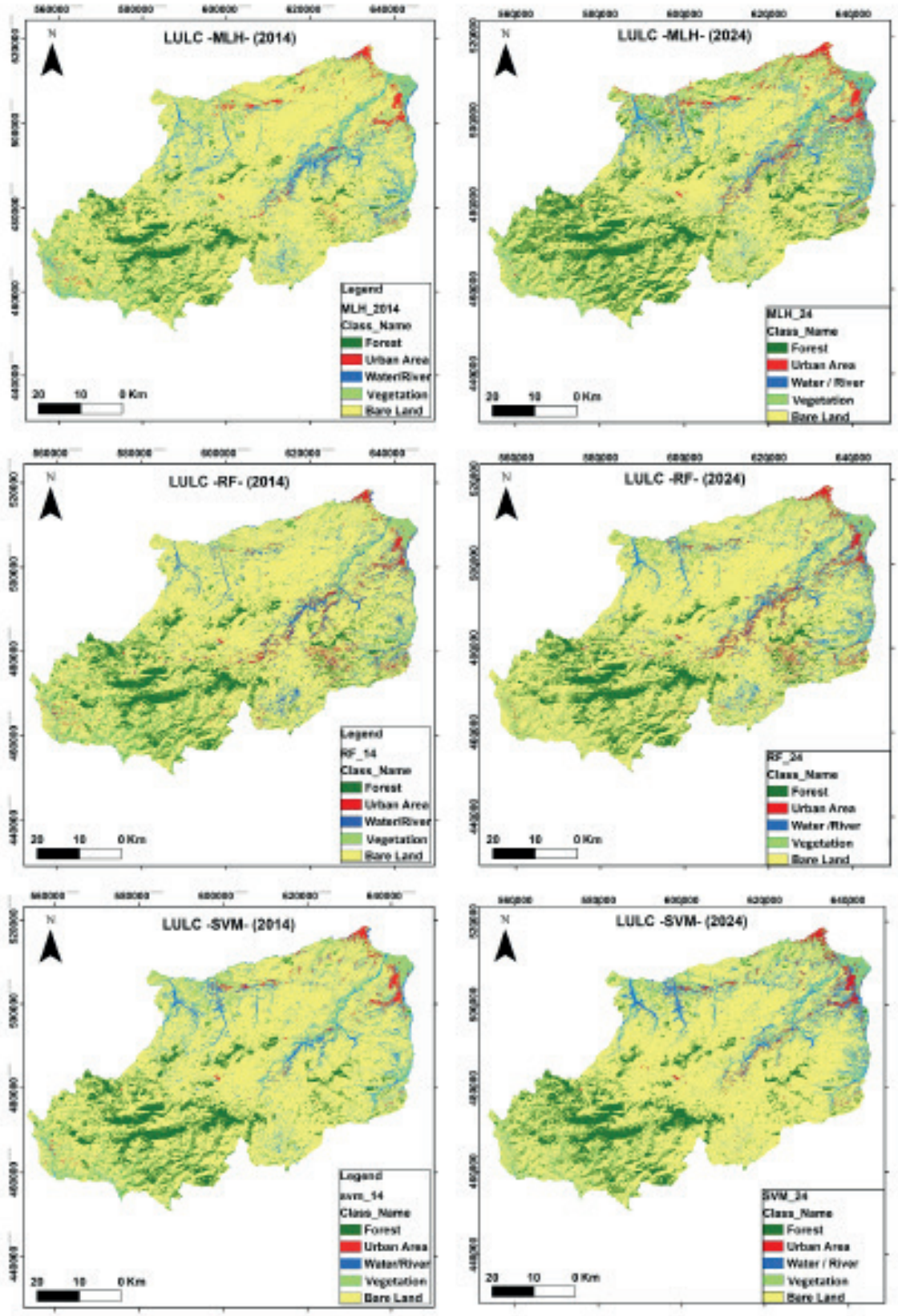

Fig. 4. LULC classification maps of Al Hoceima province for the years 2014 and 2024

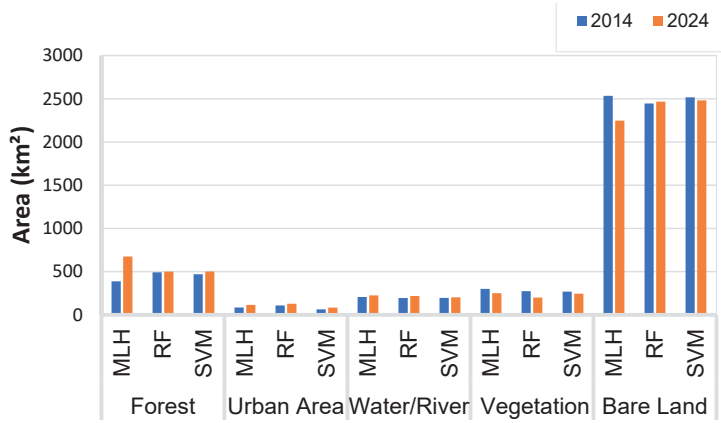

Fig. 5. Area of LULC for 2014 and 2024 according to MLH, RF and SVM algorithms

Table 4. Area change of LULC classes from 2014 to 2024 according to MLH, RF and SVM classification

Classifier	Years	Classes	Forest	Urban area	Water / River	Vegetation	Bare land
MLH	2014	km²	388	85	207	300	2534
		%	11	2	6	8	72
	2024	km²	675	115	225	250	2247
		%	19.2	3.2	6.4	7	64
	2014–2024	Changes (%)	+8.2	+1.2	+0.4	-1	-8
RF	2014	km²	492	108	194	274	2445
		%	14	3	6	8	69
	2024	km²	500	128	219	200	2466
		%	14	3.6	6	5.7	70
	2014–2024	Changes (%)	0	+0.6	0	-2.3	+1
SVM	2014	km²	469	63	196	269	2517
		%	13	1.8	6	8	71
	2024	km²	501	83	203	245	2481
		%	14	2.4	5.8	7	70.8
	2014–2024	Changes (%)	+1	+ 0.8	-0.2	-1	-0.2

classification algorithms. The obtained classification maps derived from MLH, RF and SVM classifiers are shown in Figure 4, whereas Figure 5 depicts the classification changes in km² of each class in each year throughout the study period. For all LULC classification maps through the studied period, the bare land and urban area classes have the largest and the smallest extents, respectively (Fig. 5). Starting with the MLH algorithm, the forest, urban area and water/river classes increased by 8.2%, 1.2% and 0.2%, respectively (Table 4). Conversely, vegetation and bare land classes decreased by 1% and 8%, respectively. According to the RF analysis, the forest and water/river classes

Citation: Bulletin of Geography. Physical Geography Series 2025, 29, http://doi.org/10.12775/bgeo-2025-0008

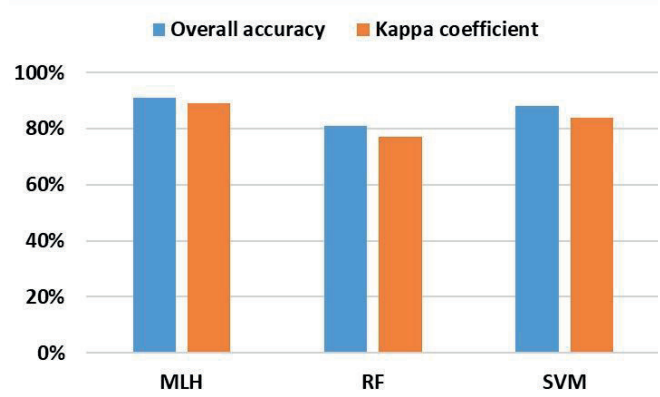

Fig. 6. Accuracy assessment of percentage

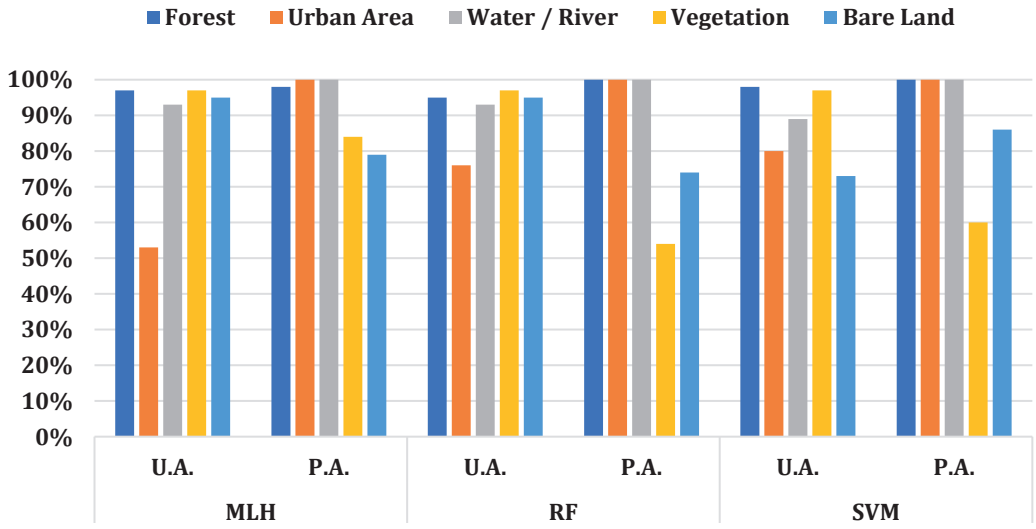

Fig. 7. Percentages of producer accuracy (PA) and user accuracy assessment (UA)

remained unchanged during the studied period 2014–24 and vegetation decreased by 2.3%, while the urban area and bare land increased by 0.6% and 1%, respectively. Regarding the SVM classification, the forest and urban area classes were increased by 1% and 0.8%, respectively, while the water/river, vegetation and bare land decreased by 0.2 %, 1% and 0.2%, respectively (Table 4).

Accuracy assessment results

The efficacy of different classifiers was evaluated through accuracy assessment, and the results are presented in Figure 6. The MLH parametric algorithm gives superior overall accuracy, achieving a rate of 91% (K = 0.89), followed by the SVM which yields an OA of 88% (K = 0.84). Finally, the RF algorithm was in the third position with an OA rate of 81% (K = 0.77). Figure 7 illustrates the user's and producer's accuracies for each classification algorithm. Across all classifiers, the UA for vegetation remains consistently high at 97%. Furthermore, both MLH and RF exhibit elevated UAs of 95% for bare land classification. Similarly, MLH and SVM demonstrate superior UAs in identifying forest cover, achieving 97% and 98%, respectively. Moreover, MLH and RF perform equally well in identifying water bodies, both achieving a UA of 93%. In terms of PA, all classifiers excel in classifying urban areas and water/river, achieving a perfect score of 100%,

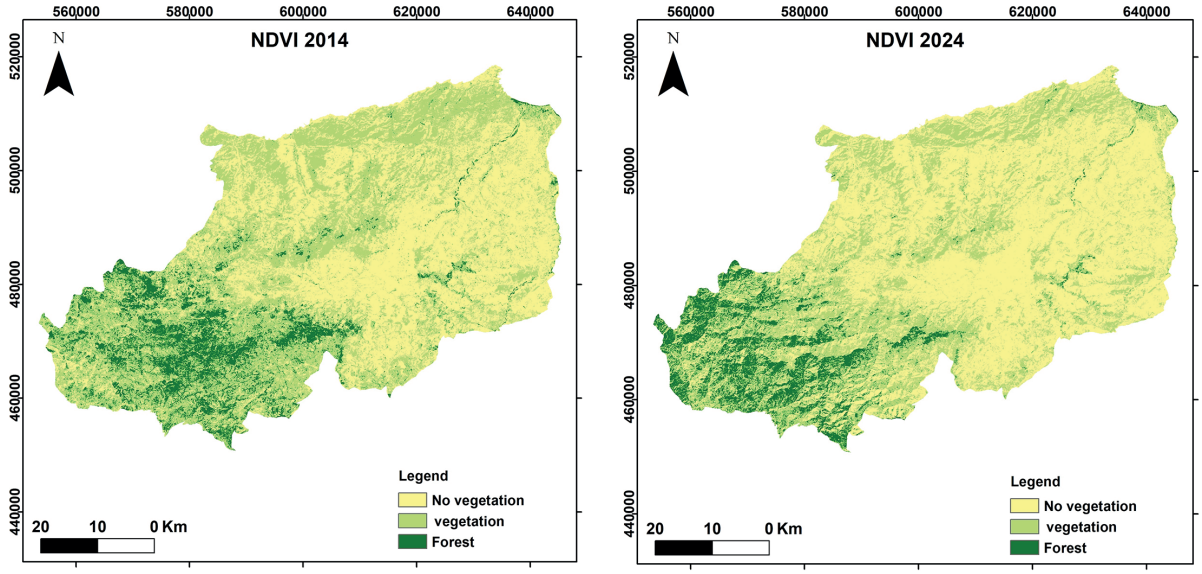

Fig. 8. NDVI maps of the years 2014 and 2024 in the study area

as well as for forest but with a PA value of 98% for MLH (Fig. 7). Conversely, MLH, RF and SVM showed lower PAs and thus struggled in accurately identifying two LULC classes: bare land (PAs were 79%, 74% and 86%, respectively) and vegetation (PAs were 84%, 54% and 60%, respectively).

NDVI changes

To determine the best result achieved by the three algorithms classifiers RF, SVM and MLH, the NDVI was determined using satellite images captured during nearly the same season. The values obtained range from –0.19 to 0.55 over the studied period (i.e., 10 years), and each map displays fluctuations in NDVI values across the study area. Based on the NDVI values, the image was divided into three distinct thematic classes according to Mohajane et al. (2018) and Ait El Haj, Ouadif and Akhssas (2023) (Fig. 8):

- No vegetation: values below 0.1, reflecting bare land
- Vegetation: values between 0.1 and 0.2, representing low-density vegetation
- Forest: NDVI higher than 0.2, regrouping moderate- and high-density vegetation

Table 5 illustrates the NDVI changes during the study period. Indeed, the no vegetation (i.e., bare land) class exhibited an increase of 12%, whereas vegetation and forest decreased by 11% and 1%, respectively. These results seem to be the closest match to the results from the RF classifier compared to other algorithms. Both NDVI and RF analyses indicated a weak change in forest class from 2014 to 2024, with vegetation declining and bare land increasing.

Table 5. NDVI changes between 2014 and 2024 in percentage

Class	NDVI range	2014 (%)	2024 (%)	Changes %
No vegetation	NDVI<0.1	46	58	+ 12
Vegetation	0.1<NDVI<0.2	43	32	-11
Forest	0.2<NDVI	11	10	-1

Citation: Bulletin of Geography. Physical Geography Series 2025, 29, http://doi.org/10.12775/bgeo-2025-0008

Discussion

LULC change in Al Hoceima province

In terms of LULC research topics, Al Hoceima province, the core of the central Rif Mountain range, is one of the most understudied areas in the northern region, or even in Morocco. In the present paper, we contributed to filling this gap by providing, for the first time, LULC maps and their spatiotemporal dynamic from 2014 to 2024 using Landsat 8 (OLI) images as inputs and three classification algorithms. LULC change mapping has been and is still largely obtained through the classification of RS data from different sensors, mainly multispectral satellite images of Landsat, MODIS and Sentinel. This classification is carried out using several methods. In the last few years, the use of machine learning algorithms has increasingly been receiving the attention of researchers worldwide.

Analyzing LULC shift in a continuous and correct manner is fundamental for sustainable development plans (Loukika et al. 2021). We mapped LULC in Al Hoceima province using three algorithms: MLH, RF and SVM. Five major LULC classes (i.e., forest, urban area, water/river, vegetation, and bare land) were identified on the generated maps (Fig. 4). Surprisingly, there are no studies dedicated to LULC assessment in Al Hoceima, except for two studies carried out on some parts of this province (i.e., the Jbel Outka Numidian massif located between Taounate and Al Hoceima provinces by El Mazi et al. (2018) and the Agni sub-catchment in Al Hoceima province by Zahnoun et al. (2023) and Allah and Abderrahim (2023)).

For the three classifiers used and both years studied, the obtained LULC maps revealed that the bare land and urban area have the largest and the smallest areas, respectively (Fig. 5). The analysis of LULC results for the period 2014–2024 showed that the study area has undergone relatively small changes, except for bare land and forest for MLH. This would be due to the short study period (one decade), which may not allow the detection of significant changes. For the three classifiers, there were two common tendencies: an increase in urban area (between 0.6% and 1.2%) and a decrease in vegetation (between –1% for both MLH and SVM and –2.3% for RF). There were two partially common tendencies between the MLH and SVM: the increase of forest class and a decrease in the bare land. The water/river class showed the most variable results for the three classifiers (increase, decrease and stability). Indeed, no changes were obtained by the RF for forest and water/river classes, MLH overestimated forest (i.e., +8.2% against only +1% for SVM). For the bare land, MLH also overestimated the changes with –8% while SVM gave a decrease of only –0.2%. Hence, both RF and SVM gave similar results for the urban area, while MLH and SVM provided identical estimation for the decreasing trend of agricultural land. Several studies reported similar results. For example, in the Ksob watershed (Western High Atlas, Morocco), Omdi, Daoudi and Adiri (2017) found an increase in barren lands and vegetated land from 1988 to 2010 and from 2010 to 2014, respectively.

Accuracy assessment

Different machine learning algorithms were used in several Earth and environmental topics such as mapping LULC changes (El Adnani et al. 2019), monitoring woody species diversity in savannas (Fundisi et al. 2022), macronutrient assessment (Misbah et al. 2022), modelling landslide susceptibility (Pacheco Quevedo et al. 2023) and erosion prediction (Aouragh et al. 2023). However, studies that compare the accuracy of two (or more) machine learning algorithms are scarce (e.g., Talukdar et al. 2020; Loukika et al. 2021; Atef et al. 2023).

In Morocco, several LULC studies performed image classification using machine learning algorithms such as SVM (e.g., El Adnani et al. 2019; Nguyen et al. 2023), RF (e.g., Acharki et al. 2022) and Spectral Angle Mapper (SAM) (e.g., Benzougagh et al. 2023). Few studies have simultaneously used several algorithms, such as Ouchra et al. (2023a), who compared six classifiers: SVM, RF Classification And Regression Trees (CART), Minimum Distance (MD), Decision Tree (DT), and Gradient Tree (GTB), and Ouchra et al. (2023b), who investigated three algorithms (RF, Boosted Regression Trees (BRT) and SVM).

Accuracy assessment gained from the validation process of the LULC classification in Al Hoceima revealed that OA and K were good to excellent (Figs 6 and 7, Appendices E and F). Numerous studies

have been carried out to obtain the best machine-learning-based algorithm for LULC classification and reported divergent performances (Oo et al. 2022). Our findings indicated that the maximum accuracy has been found for the MLH classifier (K = 0.89), followed by SVM (K = 0.84), whereas the minimum was registered for the RF algorithm (K = 0.77; Fig. 6). Our results are consistent with previous studies that used MLC, such as the study by Omdi et al. (2017), who find an OA of 100% in the western High Atlas, and Moumane et al. (2022), who reported an OA of 90% in the Anti Atlas. However, other studies reported lower accuracy of MLC in comparison with other classifiers. In the study by Atef et al. (2023) in Egypt, the SVM had the highest accuracy (0.916), followed by MLH (0.878), and RF (0.909). In the review carried out by Talukdar et al. (2020), the higher accuracy among the six classifiers they examined was 0.89 for RF and 0.86 for the SVM classifier, whereas the minimum was 0.82 for MD. Similarly, Loukika et al. (2021) found that RF had better accuracy than SVM and CART (with average Ks of 0.90, 0.84 and 0.74, respectively). Oo et al. (2022) also found that the RF gives the highest accuracy (K=0.93) followed by SVM (K=0.85) and, finally, CART and ML (K = 0.84). Ouchra et al. (2023b) found that RF is the best performing classifier (K=0.94) among the six algorithms they applied, whereas SVM gave the worst accuracy (K=0.74). Ouchra et al. (2023a) found the best accuracy with MD (K=0.93), followed by RF (K=0.89) and SVM (K=0.69).

Taking each LULC class separately, we found that the classification of urban area had the lowest UA of 53% for the MLH classifier, whereas vegetation had the lowest PA of 54% and 60% for RF and SVM, respectively. Loukika et al. (2021) also reported a lower accuracy of barren land compared to other LULC classes. Moreover, the water/river and forest classes had the highest values for all classifiers, with UA ranging from 89 to 100% and PA ranging from 98 to 100%. The varied accuracy values point to vegetation often being confused with other land cover classes (Atef et al. 2023).

Overall, for the three classifiers, we found, on the one hand, an increase in urban areas. The urban area increase indicates an expansion of uncontrolled urbanization and the development of disproportionate tourist projects (UICN 2012). Fortunately, the establishment of the Al Hoceima National Park has, for ecological purposes, made the management of a large part of the coastal area less efficient (UICN 2012). On the other hand, our results pointed to a decline in vegetation, which could be also related to the development of the tourism sector and the conservation measures related to the Al Hoceima National Park. The increase in forest cover supports this statement.

NDVI changes

In addition to classification algorithms, the use of indices such as NDVI enhances the accuracy by validating or challenging the results obtained for vegetation and forest classes. (Loukika et al. 2021; Ouchra et al. 2023a; Ouchra et al. 2023b). In our study, the NDVI maps were poorly consistent with the classification provided by the RF classifier – that is, a slight decrease in forest cover (–1% against a "no change" for RF) between 2014 and 2024 (Tables 4 and 5). Several studies have highlighted the inconsistency between machine-learning-based algorithms and indices such as NDVI in LULC classifications. Indeed, Omdi et al. (2017) found an OA of 100% for MLC against just 58% for NDVI in the western High Atlas, and they stated that NDVI was inappropriate for land cover mapping. Moreover, it has been highlighted that the usefulness of NDVI may be limited in arid and semi-arid areas (Omdi et al. 2017; Moumane et al. 2022). However, other studies have emphasized the reliability of the simultaneous use of classification algorithms with NDVI (e.g., Mohajane et al. 2018; Ouchra et al. 2023b). For instance, Ouchra et al. (2023b) pointed to the applicability of multi-temporal vegetation indices (e.g., NDVI) in numerous areas irrespective of geographical features and climatic conditions.

Many studies have reported a stability in the forest cover, such as Mohajane et al. (2018), who linked this result to good climatic conditions during the period of study (i.e., 1987–2017) and the efforts undertaken by the foresters in Azrou forest (the Central Middle Atlas). On the other hand, in a previous study, Nash et al. (2008) found a significant increase in NDVI over time (1981–2003) in the Al Hoceima region, reflected in the increase in the number and size of green patches. The authors attributed this greenness enhanced the protection of the natural resources in this region. Several studies also found an increase in NDVI

values over time in other Moroccan regions such as Barakat et al. (2018), who monitored forest cover dynamics in the eastern area of Béni-Mellal province between 2001 and 2015. This increase in forest stands was attributed to the improved protection by foresters, reforestation actions, favorable climatic conditions during the study period, the presence of microclimate reducing drought effects, and stand regeneration (Barakat et al. 2018).

Limitations of the study

Although the current study provides the first survey of LULC (urbanization, agriculture and vegetation) in Al Hoceima province, there are some limitations to be highlighted. Firstly, the application of RS techniques with small resolution (30-m for Landsat) on a small area of the study region is problematic. Secondly, the study period (2014–2024) is short and does not allow the detection of large LULC changes, which may also explain the weak consistency found between the results of classification algorithms and the NDVI. Finally, the lack of previous studies on LULC in the Al Hoceima region and lack of data constitute another factor limiting our understanding of the landscape dynamic in the study area. Indeed, a suitable interpretation of the land cover dynamics necessitates a good documentation on the study area, which was not the case in Al Hoceima; one of the most understudied regions in Morocco. Our findings represent the first LULC mapping using remote sensing-based applications in this area, which will allow deeper future investigations.

Conclusion

In the present paper, we assessed, for the first time, LULC changes in Al Hoceima province (north-eastern Morocco) over the last decade (i.e., from 2014 to 2024) using multispectral Landsat imagery and three machine learning algorithms (i.e., RF, MLH and SVM), as well as NDVI to detect vegetation changes. Accuracy level was assessed by means of the Kappa coefficient. Our main findings showed relatively small variation in the change of LULC classes among the three algorithms, mainly for urban area and agricultural land. The maximum and minimum variations were found for the bare land and forest classes, respectively. Similarly, the accuracy of LULC classification differed between the three applied algorithms. Our results reveal that the MLH classifier had the highest accuracy level in LULC classification in comparison with SVM and RF. However, the NDVI results showed weak reliability with the RF classification.

The findings of our study will offer researchers the most suitable method for LULC classification, aligning well with the specific characteristics of the study area and similar semi-arid regions exhibiting comparable features. To improve LULC classification accuracy, further research can be directed towards using deep learning algorithms such as Convolutional Neural Network (CNN). It would be also interesting to investigate other aspects such as the effect of climatic factors and drought on land cover changes. Moreover, the use of more accurate remote sensing data like Sentinel-2 images would offer detailed information on LULC evolution. Finaly, landscape evolution should be examined over a long period, by integrating information from old aerial photographs to determine the underlined factors and, thus, provide an overall picture that can help in management plans and land use policies.

Disclosure statement

No potential conflict of interest was reported by the authors.

Author contributions

Study design: MT, IE; data collection: AB, AE; statistical analysis: AB, AE; result interpretation: AM, MS; manuscript preparation: MT, IE; literature review: AM, MS .

References

ABDELKARIM A, 2023, Monitoring and Forecasting of Land Use/Land Cover (LULC) in Al-Hassa Oasis, Saudi Arabia Based on the Integration of the Cellular Automata (CA)

and the Cellular Automata-Markov Model (CA-Markov). *Geology, Ecology, and Landscapes* 00: 1–32. DOI: https://doi.org/10.1080/24749508.2022.2163741.

ACHARKI S, 2022, PlanetScope Contributions Compared to Sentinel-2, and Landsat-8 for LULC Mapping. *Remote Sensing Applications: Society and Environment* 27: 100774. DOI: https://doi.org/10.1016/j.rsase.2022.100774.

ADAM E, MUTANGA O, ODINDI J and ABDEL-RAHMAN EM, 2014, Land-Use/Cover Classification in a Heterogeneous Coastal Landscape Using (RapidEye) Imagery: Evaluating the Performance of Random Forest and Support Vector Machines Classifiers. *International Journal of Remote Sensing* 35(10): 3440–58. DOI: https://doi.org/10.1080/01431161.2014.903435.

AIT EL HAJ F, OUADIF L and AKHSSAS A, 2023, Monitoring Land Use and Land Cover Changes Using Remote Sensing Techniques and the Precipitation-Vegetation Indexes in Morocco. *Ecological Engineering and Environmental Technology* 24(1): 272–86. DOI: https://doi.org/10.12912/27197050/154937.

ALLAH Z A and ABDERRAHIM W, 2023, Spatiotemporal Evolution in Sub-Humid Region Based on Aerial Photographs and Satellite Imagery: Case Study in Agni Sub-Catchment, Northern Morocco. *Remote Sensing Applications: Society and Environment* 31: 101002.

ALSHARI EA and GAWALI B W, 2021, Development of Classification System for LULC Using Remote Sensing and GIS. Global Transitions Proceedings, 1st International Conference on Advances in Information. *Computing and Trends in Data Engineering* (AICDE-2020), 2(1): 8–17. DOI: https://doi.org/10.1016/j.gltp.2021.01.002.

AOURAGH M H, IJLIL S, ESSAHLAOUI N, ESSAHLAOUI A, EL HMAIDI A, EL OUALI A and MRIDEKH A, 2023, Remote Sensing and GIS-Based Machine Learning Models for Spatial Gully Erosion Prediction: A Case Study of Rdat Watershed in Sebou Basin, Morocco. *Remote Sensing Applications: Society and Environment* 30: 100939.

ATEF I, AHMED W and ABDEL-MAGUID RH, 2023, Modelling of Land Use Land Cover Changes Using Machine Learning and GIS Techniques: A Case Study in El-Fayoum Governorate, Egypt. *Environmental Monitoring and Assessment* 195(6). DOI: https://doi.org/10.1007/s10661-023-11224-7.

BARAKAT A, KHELLOUK R, EL JAZOULI A, TOUHAMI F and NADEM S, 2018, Monitoring of Forest Cover Dynamics in Eastern Area of Béni-Mellal Province Using ASTER and Sentinel-2A Multispectral Data. *Geology, Ecology, and Landscapes* 2(3): 203–15.

BASHEER S, WANG X, FAROOQUE AA, NAWAZ RA, LIU K, ADEKANMBI T and LIU S, 2022, Comparison of Land Use Land Cover Classifiers Using Different Satellite Imagery and Machine Learning Techniques. *Remote Sensing* 14(19): 1–18. DOI: https://doi.org/10.3390/rs14194978.

BEN-SAID M, CHEMCHAOUI A, ETEBAAI I and TAHER M, 2025, Land Use and Land Cover Changes in Morocco: Trends, Research Gaps, and Perspectives. *GeoJournal* 90(1): 44. DOI: https://doi.org/10.1007/s10708-024-11214-3.

BENZOUGAGH B, MESHRAM S G, FELLAH B E, MASTERE M, EL BASRI M, OUCHEN I, DRISS S, BAMMOU Y, MOUTAOIKIL N and TURYASINGURA B, 2024, Mapping of Land Degradation Using Spectral Angle Mapper Approach (SAM): The Case of Inaouene Watershed (Northeast Morocco). *Modeling Earth Systems and Environment* 10(1): 221–31.

BOURJILA A, DIMANE F, GHALIT M, TAHER M, KAMARI S, EL HAMMOUDANI Y, ACHOUKHI I and HABOUBI K, 2023, Mapping the Spatiotemporal Evolution of Seawater Intrusion in the Moroccan Coastal Aquifer of Ghiss-Nekor Using GIS-Based Modeling. *Water Cycle* 4: 104–19. DOI: https://doi.org/10.1016/j.watcyc.2023.05.002.

BOURJILA A, DIMANE F, NOUAYTI N, TAHER M, and EL OUARGHI H, 2020, Use of GIS, Remote Sensing and AHP Techniques to Delineate Groundwater Potential Zones in the Nekor Basin, Central Rif of Morocco. In: *Proceedings of the 4th Edition of International Conference on Geo-IT and Water Resources 2020, Geo-IT and Water Resources* 2020, 1–7.

BOURJILA A, DIMANE F, OUARGHI HE, NOUAYTI N, TAHER M, HAMMOUDANI YE, SAADI O and BENSIALI A, 2021, Groundwater Potential Zones Mapping by Applying GIS, Remote Sensing and Multi-Criteria Decision Analysis in the Ghiss Basin, Northern Morocco. *Groundwater for Sustainable Development* 15: 100693.

CHAVES EDM, PICOLI CAM and SANCHES DI, 2020, Recent Applications of Landsat 8/OLI and Sentinel-2/MSI for Land Use and Land Cover Mapping: A Systematic Review. *Remote Sensing* 12(18): 3062. DOI: https://doi.org/10.3390/rs12183062.

CHIRICI G, MURA M, MCINERNEY D, PY N, TOMPPO EO, WASER LT, TRAVAGLINI D and MCROBERTS RE, 2016, A Meta-Analysis and Review of the Literature on the k-Nearest Neighbors Technique for Forestry Applications That Use Remotely Sensed Data. *Remote Sensing of Environment* 176: 282–94. DOI: https://doi.org/10.1016/j.rse.2016.02.001.

CHOWDHURY MS, 2024a, Comparison of Accuracy and Reliability of Random Forest, Support Vector Machine, Artificial Neural Network and Maximum Likelihood Method in Land Use/Cover Classification of Urban Setting. *Environmental Challenges* 14: 100800. DOI: https://doi.org/10.1016/j.envc.2023.100800.

CHOWDHURY MS, 2024b, Comparison of Accuracy and Reliability of Random Forest, Support Vector Machine, Artificial Neural Network and Maximum Likelihood Method in Land Use/Cover Classification of Urban Setting. *Environmental Challenges* 14: 100800. DOI: https://doi.org/10.1016/j.envc.2023.100800.

CHU M, LU J and SUN D, 2022, Influence of Urban Agglomeration Expansion on Fragmentation of Green Space: A Case Study of Beijing-Tianjin-Hebei Urban Agglomeration. *Land* 11(2): 275. DOI: https://doi.org/10.3390/land11020275.

DAUNT ABP, INOSTROZA L and HERSPERGER AM, 2021, The Role of Spatial Planning in Land Change: An Assessment of Urban Planning and Nature Conservation Efficiency at the Southeastern Coast of Brazil. *Land Use Policy* 111: 105771. DOI: https://doi.org/10.1016/j.landusepol.2021.105771.

DIBS H, HASAB HA, AL-RIFAIE JK and AL-ANSARI N, 2020, An Optimal Approach for Land-Use / Land-Cover Mapping by Integration and Fusion of Multispectral Landsat OLI Images: Case Study in Baghdad, Iraq. *Water, Air, & Soil Pollution* 231(9): 488. DOI: https://doi.org/10.1007/s11270-020-04846-x.

EL ADNANI A, HABIB A, EL KHALIDI K and ZOURARAH B, 2019, Spatio-Temporal Dynamics and Evolution of Land Use Land Cover Using Remote Sensing and GIS in Sebou Estuary, Morocco. *Journal of Geographic Information System* 11(5): 551–66. DOI: https://doi.org/10.4236/jgis.2019.115034.

ERRAHMOUNI A, EL MESSARI JES and TAHER M, 2022, Estimation of Groundwater Recharge Using APLIS Method – Case Study of Bokoya Massif (Central Rif, Morocco). *Ecological Engineering and Environmental Technology* 23(4): 57–66. DOI: https://doi.org/10.12912/27197050/149956.

FRIMPONG BF, KORANTENG A, ATTA-DARKWA T, JUNIOR OF and ZAWIŁA-NIEDŹWIECKI T, 2023, Land Cover Changes Utilising Landsat Satellite Imageries for the Kumasi Metropolis and Its Adjoining Municipalities in Ghana (1986–2022). *Sensors* 23(5): 2644. DOI: https://doi.org/10.3390/s23052644.

FUNDISI E, TESFAMICHAEL SG and AHMED F, 2022, Remote Sensing of Savanna Woody Species Diversity: A Systematic Review of Data Types and Assessment Methods. *PLoS ONE* 17: 1–29. DOI: https://doi.org/10.1371/journal.pone.0278529.

GISLASON PO, BENEDIKTSSON JA and SVEINSSON JR, 2006, Random Forests for Land Cover Classification. *Pattern Recognition Letters* 27(4): 294–300.

GONG W, LIU T, DUAN X, SUN Y, ZHANG Y, TONG X and QIU Z, 2022, Estimating the soil erosion response to land-use land-cover change using GIS-based RUSLE and remote sensing: a case study of miyun reservoir, north China. *Water* 14(5): 742.

GXOKWE S, DUBE T and MAZVIMAVI D, 2023, An Assessment of Long-Term and Large-Scale Wetlands Change Dynamics in the Limpopo Transboundary River Basin Using Cloud-Based Earth Observation Data. *Wetlands Ecology and Management* 32: 89-108. DOI: https://doi.org/10.1007/s11273-023-09963-y.

HASAN MM, NILAY MSM, JIBON NH and RAHMAN RM, 2023, LULC Changes to Riverine Flooding: A Case Study on the Jamuna River, Bangladesh Using the Multilayer Perceptron Model. *Results in Engineering* 18: 101079. DOI: https://doi.org/10.1016/j.rineng.2023.101079.

HASAN NA, YANG D and AL-SHIBLI F, 2023, A Historical–Projected Analysis in Land Use/Land Cover in Developing Arid Region Using Spatial Differences and Its Relation to the Climate. *Sustainability* (Switzerland) 15(3): 2821. DOI: https://doi.org/10.3390/su15032821.

HCP. 2017. Monographie Provinciale. Edited by High Commission for Planning. Monographi.

HOSSAIN MS, KHAN MAH, OLUWAJUWON TV, BISWAS J, RUBAIOT ABDULLAH SM, TANVIR MSSI, MUNIRA S and CHOWDHURY MNA, 2023, Spatiotemporal Change Detection of Land Use Land Cover (LULC) in Fashiakhali Wildlife Sanctuary (FKWS) Impact Area, Bangladesh, Employing Multispectral Images and GIS. *Modeling Earth Systems and Environment* 9(3): 3151–73. DOI: https://doi.org/10.1007/s40808-022-01653-7.

HU Y, RAZA A, SYED NR, ACHARKI S, RAY RL, HUSSAIN S, DEHGHANISANIJ H, ZUBAIR M and ELBELTAGI A, 2023, Land Use/Land Cover Change Detection and NDVI Estimation in Pakistan's Southern Punjab Province. *Sustainability* (Switzerland) 15(4): 3572. DOI: https://doi.org/10.3390/su15043572.

IENCO D, INTERDONATO R, GAETANO R and MINH DHT, 2019, Combining Sentinel-1 and Sentinel-2 Satellite Image Time Series for Land Cover Mapping via a Multi-Source Deep Learning Architecture. *ISPRS Journal of Photogrammetry and Remote Sensing* 158: 11–22.

JUNAID M, SUN J, IQBAL A, SOHAIL M, ZAFAR S and KHAN A, 2023, Mapping LULC Dynamics and Its

Potential Implication on Forest Cover in Malam Jabba Region with Landsat Time Series Imagery and Random Forest Classification. *Sustainability* (Switzerland) 15(3): 1858. DOI: https://doi.org/10.3390/su15031858.

KRUASILP J, PATTANAKIAT S, PHUTTHAI T, VARDHANABINDU P and NAKMUENWAI P, 2023, Evaluation of Land Use Land Cover Changes in Nan Province, Thailand, Using Multi-Sensor Satellite Data and Google Earth Engine. *Environment and Natural Resources Journal* 21(2): 186–97. DOI: https://doi.org/10.32526/ennrj/21/202200200.

KUMAR A and GORAI AK, 2023, A Comparative Evaluation of Deep Convolutional Neural Network and Deep Neural Network-Based Land Use/Land Cover Classifications of Mining Regions Using Fused Multi-Sensor Satellite Data. *Advances in Space Research* 72(11): 4663–76. DOI: https://doi.org/10.1016/j.asr.2023.08.057.

LAVANYA K, MAHENDRAN A, SELVANAMBI R, MAZZARA M and HEMANTH JD, 2023, Tunicate Swarm Algorithm with Deep Learning Based Land Use and Cover Change Detection in Nallamalla Forest India. *Applied Sciences* (Switzerland) 13(2): 1173. DOI: https://doi.org/10.3390/app13021173.

LEKKA C, PETROPOULOS GP and DETSIKAS SE, 2024, Appraisal of EnMAP Hyperspectral Imagery Use in LULC Mapping When Combined with Machine Learning Pixel-Based Classifiers. *Environmental Modelling & Software* 173: 105956. DOI: https://doi.org/10.1016/j.envsoft.2024.105956.

LOUKIKA KN, KEESARA VR and SRIDHAR V, 2021, Analysis of Land Use and Land Cover Using Machine Learning Algorithms on Google Earth Engine for Munneru River Basin, India. *Sustainability* (Switzerland) 13(24): 13758. DOI: https://doi.org/10.3390/su132413758.

MANSOUR S, GHONEIM E, EL-KERSH A, SAID S and ABDELNABY S, 2023, Spatiotemporal Monitoring of Urban Sprawl in a Coastal City Using GIS-Based Markov Chain and Artificial Neural Network (ANN). *Remote Sensing* 15(3): 1–24. DOI: https://doi.org/10.3390/rs15030601.

MAZI ME, SABER E and HOUARI A, 2018, Spatial and Temporal Evolution of Forests Ecosystems in the Numidian Massif of the Rif Range (Morocco): Case of Jbel Outka Evolution Spatio-Temporelle Des Écosystèmes Forestiers Dans Les Massifs Numidiens de La Chaîne Rifaine (Maroc): Cas de Jbel Outka. *Geo-Eco-Trop* 42 (1): 133–45.

MCHUGH ML, 2012, Interrater Reliability: The Kappa Statistic. *Biochemia Medica* 22(3): 276–82.

MIRMAZLOUMI SM, KAKOOEI M, MOHSENI F, GHORBANIAN A, AMANI M, CROSETTO M and MONSERRAT O, 2022, ELULC-10, a 10 m European Land Use and Land Cover Map Using Sentinel and Landsat Data in Google Earth Engine. *Remote Sensing* 14(13): 1–27. DOI: https://doi.org/10.3390/rs14133041.

MISBAH K, LAAMRANI A, KHECHBA K, DHIBA D and CHEHBOUNI A, 2022, Multi-Sensors Remote Sensing Applications for Assessing, Monitoring, and Mapping Npk Content in Soil and Crops in African Agricultural Land. *Remote Sensing* 14(1): 81. DOI: https://doi.org/10.3390/rs14010081.

MOHAJANE M, ESSAHLAOUI ALI, OUDIJA F, EL HAFYANI ME, EL HMAIDI AE, EL OUALI AE, RANDAZZO G and TEODORO AC, 2018, Land Use/Land Cover (LULC) Using Landsat Data Series (MSS, TM, ETM+ and OLI) in Azrou Forest, in the Central Middle Atlas of Morocco. *Environments* 5(12): 131. DOI: https://doi.org/10.3390/environments5120131.

MOUMANE A, AL KARKOURI J, BENMANSOUR A, EL GHAZALI FE, FICO J, KARMAOUI A and BATCHI M, 2022, Monitoring Long-Term Land Use, Land Cover Change, and Desertification in the Ternata Oasis, Middle Draa Valley, Morocco. *Remote Sensing Applications: Society and Environment* 26: 100745.

NASH MS, CHALOUD DJ, KEPNER WG and SARRI S, 2008, Morocco Case Study (1981–2003). *Environmental Change and Human Security: Recognizing and Acting on Hazard Impacts*, 143.

NGUYEN TT, ADERDOUR N, RHINANE H and BUERKERT A, 2023, Vegetation Cover Dynamics in the High Atlas Mountains of Morocco. *Remote Sensing* 15(5): 1366. DOI: https://doi.org/10.3390/rs15051366.

OMDI FE, DAOUDI L and ADIRI Z, 2017, Land Cover Changes in the Ksob Watershed (Western High Atlas, Morocco) *Using Remote Sensing Techniques* 8(10): 2229-5518.

OO TK, ARUNRAT N, SEREENONCHAI S, USSAWARUJIKULCHAI A, CHAREONWONG U and NUTMAGUL W, 2022, Comparing Four Machine Learning Algorithms for Land Cover Classification in Gold Mining: A Case Study of Kyaukpahto Gold Mine, Northern Myanmar. *Sustainability* (Switzerland) 14(17): 10754. DOI: https://doi.org/10.3390/su141710754.

OUCHRA H, BELANGOUR A and ERRAISSI A, 2023a, *Machine Learning Algorithms for Satellite Image Classification Using Google Earth Engine and Landsat Satellite Data: Morocco Case Study*. IEEE Access.

OUCHRA H, BELANGOUR A, ERRAISSI A and BANANE M, 2023b, Assessing Machine Learning Algorithms for

Land Use and Land Cover Classification in Morocco Using Google Earth Engine. In: *International Conference on Image Analysis and Processing*, 395–405. Springer.

PACHECO QUEVEDO R, VELASTEGUI-MONTOYA A, MONTALVÁN-BURBANO N, MORANTE-CARBALLO F, KORUP O and DALELES RENNÓ C, 2023, Land Use and Land Cover as a Conditioning Factor in Landslide Susceptibility: A Literature Review. *Landslides* 20(5): 967–82.

PANDEY DK, HUNJRA AI, BHASKAR R and AL-FARYAN MAS, 2023, Artificial Intelligence, Machine Learning and Big Data in Natural Resources Management: (A) Comprehensive Bibliometric Review of Literature Spanning 1975–2022. *Resources Policy* 86: 104250. DOI: https://doi.org/10.1016/j.resourpol.2023.104250.

PHAN TN, KUCH V and LEHNERT LW, 2020, Land Cover Classification Using Google Earth Engine and Random Forest Classifier—The Role of Image Composition. *Remote Sensing* 12(15): 2411. DOI: https://doi.org/10.3390/rs12152411.

SHETTY S, GUPTA PK, BELGIU M and SRIVASTAV SK, 2021, Assessing the Effect of Training Sampling Design on the Performance of Machine Learning Classifiers for Land Cover Mapping Using Multi-Temporal Remote Sensing Data and Google Earth Engine. *Remote Sensing* 13(8): 1433. DOI: https://doi.org/10.3390/rs13081433.

SISAY G, GESSESSE B, FÜRST C, KASSIE M and KEBEDE B, 2023, Modeling of Land Use/Land Cover Dynamics Using Artificial Neural Network and Cellular Automata Markov Chain Algorithms in Goang Watershed, Ethiopia. *Heliyon* 9(9): e20088. DOI: https://doi.org/10.1016/j.heliyon.2023.e20088.

TAHER M, MOURABIT T, ERRAHMOUNI A and BOURJILA A, 2023, New Tectonic and Topometric Evidence of Modern Transtensional Tectonics in the Low Nekor Basin (NE Morocco). *Advances in Science, Technology and Innovation*, 175–78. DOI: https://doi.org/10.1007/978-3-031-43222-4_38.

TAHER M, MOURABIT T, ETEBAAI I, DEKKAKI H C, AMARJOUF N, AMINE A, ABDELHAK B, ERRAHMOUNI A and AZZOUZI S, 2023, Identification of groundwater potential zones (GWPZ) Using geospatial techniques and AHP method: A case study of the Boudinar Basin, Rif Belt (Morocco). *Geomatics and Environmental Engineering* 17(3): 83–106.

TAHER M, MOURABIT T, BOURJILA A, SAADI O, ERRAHMOUNI A, EL MARZKIOUI F and EL MOUSAOUI M, 2022, An Estimation of Soil Erosion Rate Hot Spots by Integrated USLE and GIS Methods: A Case Study of the Ghiss Dam and Basin in Northeastern Morocco. *Geomatics and Environmental Engineering* 16(2): 95–110. DOI: https://doi.org/10.7494/geom.2022.16.2.95.

TAHER M, MOURABIT T, EL TALIBI H, ETEBAAI I, BOURJILA A, ERRAHMOUNI A and LAMGHARBAJ M, 2022, The Risk Mapping of Coastal Flooding Areas Due to Tsunami Wave Run-Up Using DAS Model and Its Impact on Nekor Bay (Morocco). *Ecological Engineering and Environmental Technology* 23(4): 136–48. DOI: https://doi.org/10.12912/27197050/150310.

TALUKDAR S, SINGHA P, MAHATO S, PAL S, LIOU YA and RAHMAN A, 2020, Land-use land-cover classification by machine learning classifiers for satellite observations—A review. *Remote sensing* 12(7): 1135. DOI: https://doi.org/10.3390/rs12071135.

TASSI A, GIGANTE D, MODICA G, DI MARTINO L and VIZZARI M, 2021, Pixel-vs. Object-Based Landsat 8 Data Classification in Google Earth Engine Using Random Forest: The Case Study of Maiella National Park. *Remote Sensing* 13(12): 2299. DOI: https://doi.org/10.3390/rs13122299.

UICN, 2012, Union Internationale Pour La Conservation de La Nature et de Ses Ressources (UICN) (nternational Union for Conservation of Nature and Natural Resources (IUCN) – in French), 6–26.

VERDE N, KOKKORIS I P, GEORGIADIS C, KAIMARIS D, DIMOPOULOS P, MITSOPOULOS I and MALLINIS G, 2020, National Scale Land Cover Classification for Ecosystem Services Mapping and Assessment, Using Multitemporal Copernicus EO Data and Google Earth Engine. Remote Sensing 12(20): 1–24. DOI: https://doi.org/10.3390/rs12203303.

WANG Y, SUN Y, CAO X, WANG Y, ZHANG W and CHENG X, 2023, A Review of Regional and Global Scale Land Use/Land Cover (LULC) Mapping Products Generated from Satellite Remote Sensing. *ISPRS Journal of Photogrammetry and Remote Sensing* 206: 311–34. DOI: https://doi.org/10.1016/j.isprsjprs.2023.11.014.

WULDER MA, COOPS NC, ROY DP, WHITE JC and HERMOSILLA T, 2018a, Land Cover 2.0. *International Journal of Remote Sensing* 39(12): 4254–84. DOI: https://doi.org/10.1080/01431161.2018.1452075.

Received 27 April 2025
Accepted 30 June 2025